Production of energetic positronium at metal surfaces

R. H. Howell, I. J. Rosenberg, and M. J. Fluss
Lawrence Livermore National Laboratory, Livermore, California 94550
(Received 3 March 1986)

The production of positronium with kinetic energy greater than the positronium negative work function is clearly shown by time-of-flight spectroscopy of annihilating triplet positronium produced by the bombardment of low-energy positrons on metals. This higher-energy positronium channel is believed to be a consequence of positrons inelastically backscattered through the metal surface. At positron bombarding energies less than 100 eV, the positronium produced from backscattered positrons can be more intense than that produced by the diffusion of thermalized positrons to the surface.

INTRODUCTION

There are two previously identified mechanisms for producing positronium at metal surfaces: positronium emission as a consequence of a negative positronium work function,[1] yielding a kinetic-energy distribution of positronium up to the work-function energy; and thermal desorption of positronium from positrons bound at the metal surface leading to a temperature dependence in the yield and positronium kinetic energies typical of a thermal process.[2] Both the work-function emission (work-function positronium) and the thermal desorption of positronium are sensitive to the diffusion of thermalized or nearly thermalized positrons to the surface as well as the condition of the surface itself. The change in the probability that implanted positrons will diffuse back to the surface has been used by several investigators to study the depth-dependent phase and defect properties of metallic samples.[3] Such experiments have used the fraction of positrons annihilating as positronium as a scale of the number of positrons diffusing to the sample surface. Although low-energy incident positrons are sometimes used, the possibility of a large positronium signal as a consequence of backscattered positrons has been ignored.

We are reporting measurements of positronium at metal surfaces with kinetic energies significantly greater than those available from the negative work-function energy for positronium. We believe this positronium is formed when positrons that backscatter from the sample pick up an electron as they pass through the surface (backscatter positronium). In this paper we will refer to the two types of positronium by the method of emission of the positron, i.e., work-function or backscatter positronium.

It is expected that some fraction of positrons at low energies will emerge from metals without thermalization, since this effect has been both observed experimentally and predicted in calculations.[4,5] These observations confirm the early suggestion of Brandt that positronium formed with very-low-energy beams resulted from backscattered positrons.[6] They are the first direct observations that a large fraction of these positrons capture an electron and efficiently form high-energy positronium.

EXPERIMENT

Positronium time-of-flight data were taken using the intense, pulsed, variable monoenergetic positron beam from the Lawrence Livermore National Laboratory 100-MeV Electron Linac.[7] The positron beam was transported at 1440 pulses per second with a 15-ns duration and a kinetic energy of 500 eV. The positron energy at the sample could be varied between 0—3000 eV by adjusting the bias on the sample. The maximum number of positrons per pulse (7×10^4) was chosen to avoid distortion of the spectra due to multiple counts in the detectors during a single pulse. The positronium time of flight was determined by measuring the time difference between the positron beam arrival and γ rays from the decay of free, long-lived, triplet positronium. The time-of-flight detector was collimated by a 0.7-cm-wide slit to view a planar volume 10.5 cm from the sample surface, as shown in Fig. 1. Also, as shown in Fig. 1, detectable positronium leaving the sample surface was constrained by a circular collimator to a maximum angle of 30° from the normal of the sample surface. Total positron decay rates and the fraction of triplet positronium were monitored in lifetime measurements made with a separate plastic scintillation detector placed to have an unobstructed view of the sample and surrounding volume.

Experiments were performed in an ultrahigh-vacuum chamber having 1×10^{-10} Torr base pressure. Single-crystal metal samples of Al(111), Cu(100), Ni(100), and Au(100), with the surface cut along the indicated low-index plane, were obtained from commercially available sources. Each sample was argon-ion sputtered at 3 keV, *in situ*, at an oblique angle of incidence, and annealed in repeated cycles until surface contamination, observed by Auger analysis, was minimized (usually less than 10 at.%). Since the typical time for a measurement was 10—20 min, contamination build-up during the runs was not a problem. Near-surface defects were introduced into the samples for some of the measurements by raising the argon-ion energy to 5 keV and measuring without annealing. Positronium time-of-flight and lifetime spectra were obtained for incident positron energies from 50 eV to 3

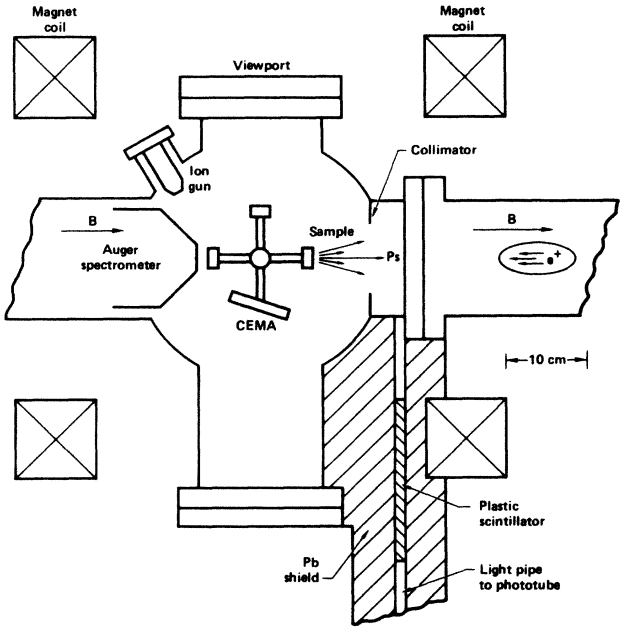

FIG. 1. A schematic representation of the time-of-flight detection system used at the Lawrence Livermore National Laboratory 100-MeV Electron Linac to measure the time-of-flight distribution of triplet positronium. The pulsed positronium beam enters the target chamber from the right with an energy of 500 eV. The energy of the positrons at the sample is then varied by changing the voltage of the sample relative to ground. Emitted positronium is constrained to a cone with an opening angle of 60° and is shown traveling to the right. Only the fraction of positronium that annihilates in the collimated view of the shielded detector is detected, but there is a significant background from γ rays from other sources scattering into the detector.

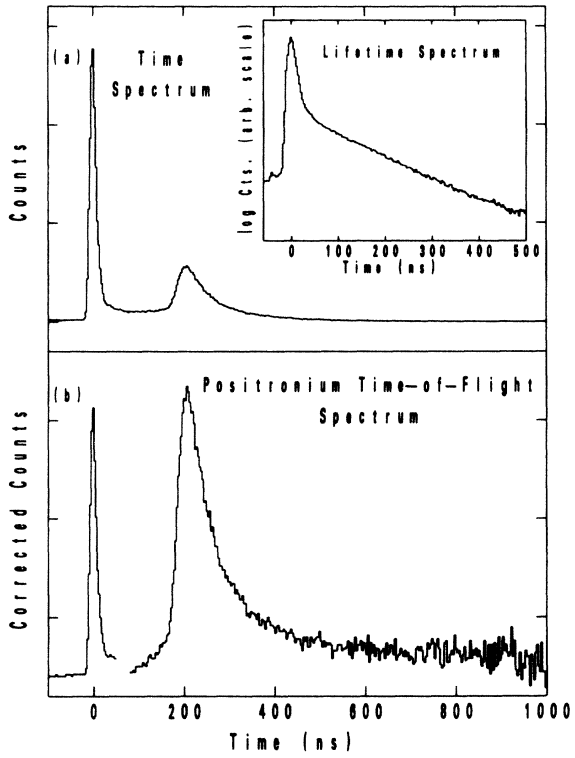

FIG. 2. (a) A spectrum of the time distribution of detected γ rays for 2-keV positrons incident on a Au(100) target. The prompt γ rays from annihilation of singlet positronium, and positrons in or at the surface of the sample is seen at the left. The width of this peak is indicative of the overall instrumental resolution and its position serves as a fiducial time mark for arrival of the pulsed positron beam. (b) The same spectrum, background subtracted and corrected for the decay of triplet positronium in flight and residence time in front of the time-of-flight detector. The background from scattered γ rays from triplet positronium decay has been subtracted from the time-of-flight distribution. (inset) A lifetime spectrum taken simultaneously with the time-of-flight spectrum. The short component is prompt and singlet decay of positrons and positronium; the long component is triplet positronium decay. Total positron annihilation rates and positronium fractions were derived from this data to monitor the course of the experiment and to normalize the final results.

keV; the running time and total linac electron beam charge were also recorded for each run. A typical raw data spectrum contains between 300 and 1000 counts in a 1-ns bin at the peak of the positronium distribution.

Time-of-flight data for Cu bombarded with 2-keV positrons are shown in Fig. 2. Figure 2(a) is the time distribution of detected γ rays for the as-collected spectrum, and Fig. 2(b) is the same data corrected for the decay in flight of the positronium and the detector efficiency. Thus, the corrected spectrum maps the velocity distribution of positronium as it leaves the sample to the distribution of positronium flight times. The narrow peak at the left of this spectrum arises from the detection of scattered γ rays produced from the prompt annihilation of positrons and singlet positronium at or near the surface of the sample. The shape of this prompt peak is indicative of the overall timing resolution of the production, transport, and timing circuitry, and its location zero time. The detection of annihilation gamma rays arising from the decay of the long-lived triplet positronium in the field of view of the detector is seen in the spectrum at later times along with a background resulting from scattered γ rays from triplet positronium annihilating outside the detector field of view.

The spectrum in Fig. 2(b) has been transformed from a time distribution of detected γ rays into a time-of-flight distribution of positronium by applying the following corrections. A time-independent, random background, determined from the count rate taken at long times, was subtracted, and then the data for both the scattered and directly detected γ rays (excluding the prompt peak) were corrected for the decay of positronium by multiplying each channel by $\exp[t/(142\text{ ns})]$, where t is the time from the prompt-peak zero. This results in a positronium time-of-flight distribution and a uniform flat background from scattered triplet-state γ rays. After subtracting the flat background from the positronium time-of-flight distribution, an additional correction proportional to $1/t$ is required to compensate for the velocity dependence in the time a positronium spends in front of the active region of the detector.

The inset in Fig. 2(a) shows a lifetime spectrum typical of those collected simultaneously with each time-of-flight spectrum. The spectrum contains two components; a short-lived one from the decay of a mixture of singlet positronium and positrons remaining at or in the sample, and a long-lived component from the decay of triplet positronium. These data were reduced to the relative intensities of the short- and long-lived components. Since the long lifetime is uniquely associated with triplet positronium, the fraction of positronium annihilations and the total number of detected positron annihilations in any state can be calculated from the long and short intensities and the detection efficiency of the short component relative to the long one. The relative efficiency was determined by noting that for samples where all positions annihilate at the sample producing different amount of positronium the distribution of the counting rate of short-lived events with respect to the counting rate of long-lived events falls on a straight line with a slope determined by the relative detection efficiency. This method was used to determine the value of the efficiency used in the positronium fraction and total annihilation calculations.

RESULTS

At higher incident positron energies the dominant method for the production of positronium at metal surfaces is due to the expulsion of electron-positron pairs by the negative work function for the bound positron system. This occurs when a thermalized positron and an electron from the Fermi distribution bind together, resulting in sufficient excess energy so that the positronium system can escape the material. The work-function mechanism for producing positronium results in a distribution of positronium energies that is clearly identified in positronium velocity spectroscopy, as seen in Fig. 3. Work-function values have been determined from high-positron-energy data and are in good agreement with those calculated from the electron and positron work functions and the positronium binding energy. Details of these comparisons of the technique for determining the work functions and the shape of the work-function spectra are found in Ref. 8.

The main features in the positronium time-of-flight distributions in Figs. 2 and 3 are a peak from fast annihilations at the sample and a flat background from delayed positronium annihilations, both from scattered γ rays, and the work-function peak. The edge of the peak at short time corresponds to the most energetic positronium, i.e., that with the full energy available from the negative work function. The distribution of positronium to longer flight times corresponds to lower-energy positronium resulting from positronium formation with more tightly-bound electrons. It has been suggested that the shape of the positronium peak can be related to the electron density of states;[1] this proposal will be discussed with regard to these data in a future publication. In a few cases, a second, small prompt peak, due to a satellite electron pulse from the electron linac, was seen. The satellite prompt peak has been subtracted from those spectra where it overlaps the positronium data.

Backscattering that produces positronium is a pronounced additional feature when the energy of the positron beam is low enough that many positrons scatter through the surface without thermalization. The effect is very large at low energies, as is seen in Fig. 3. At 50 eV, the positron energy is low enough that the positron mean free path, 5 Å, is similar to its penetration depth, 5 Å,[9] and some positrons may scatter back in a single interaction. The striking feature of the low-energy spectra is not that there is a significant positron backscatter but that the backscatter produces positronium with higher efficiencies than the work function. For those spectra where the positrons are deeply implanted, the backscatter channel for the production of positronium is minor, but detectable. It is seen as a high-energy tail (short time) on the work-function positronium spectrum.

To demonstrate that the mechanism that results in the formation of positronium with kinetic energies greater than the work function is not diffusion limited, it is possible to disrupt the migration of thermal positrons to the surface and thus reduce the intensity of the work-function

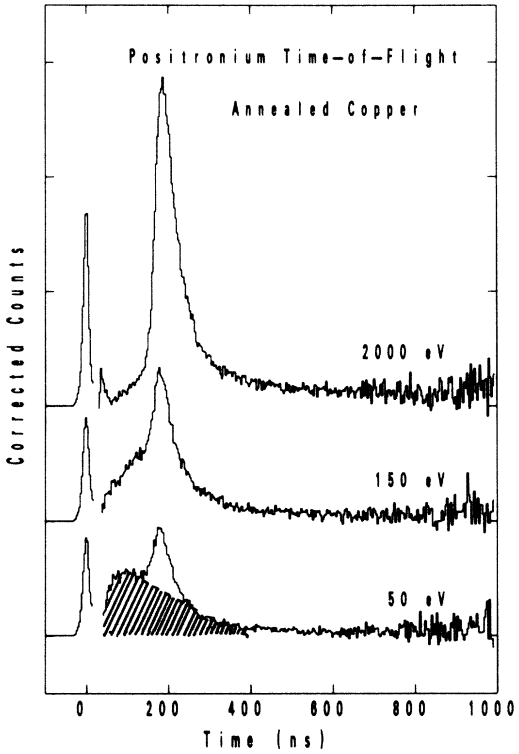

FIG. 3. Time-of-flight spectra taken on a clean well annealed Cu sample for initial positron energies of 2000, 150, and 50 eV. Positronium formed by thermal positrons and conduction electrons expelled by the negative positronium work function is the main feature in the 2-keV spectrum, however, some positronium from backscattered positrons is evident in the shaded region. At lower initial positron energies, the contribution to positronium formation from backscattered positrons becomes large. The second, small prompt peak in the 2000-eV spectrum is due to a satellite electron pulse in the electron linac beam during one experiment. The satellite prompt peak has been subtracted from those lower energy spectra where it overlaps the positronium data.

positronium channel. This effect is seen in Fig. 4 where ion bombardment of the sample by 5-keV Ar ions has introduced bulk trapping sites for diffusing positrons that attenuate the diffusion of thermal positrons to the surface and reduce the strength of the work-function positronium without changing the shape of the distribution.

Sputter damage of the surface reduces the strength of the positronium produced by the work-function mechanism, but neither the energy distribution nor the intensity of the positronium produced from backscattered positrons is significantly affected by the disruption of the surface by sputtering, as seen by comparison of the spectra in Figs. 3 and 4. Positron trapping sites change the work-function intensity by trapping positrons prior to reaching the surface resulting in a diminished yield of work-function positronium and a greater yield of prompt annihilations from the bulk of the sample. We have already seen that work-function positronium production is inhibited in sputtered samples at high positron energies. Sputtering the material disrupts the formation of work-function positronium at low incident positron energies as well. It is easy to distinguish between positronium formed from thermalized positrons, that are limited by positron diffusion, and positronium formed from backscattered positrons that are not limited by diffusion and form higher kinetic energy positronium. The yield and spectral shape of the backscattered limited positronium was observed to be independent of whether the sample was sputter damaged or annealed for all incident positron energies.

Since the sputter damage reduces the intensity of the work-function positronium without affecting the backscatter positronium, it is convenient to compare the positronium energy distributions of the sputtered samples. Although a contribution due to work-function positronium is still evident in these spectra, the strength is low enough to allow the shape of the underlying backscattered produced positronium to be seen. The comparison of such spectra for several positron incident energies between 2000 and 50 eV is shown in Fig. 4.

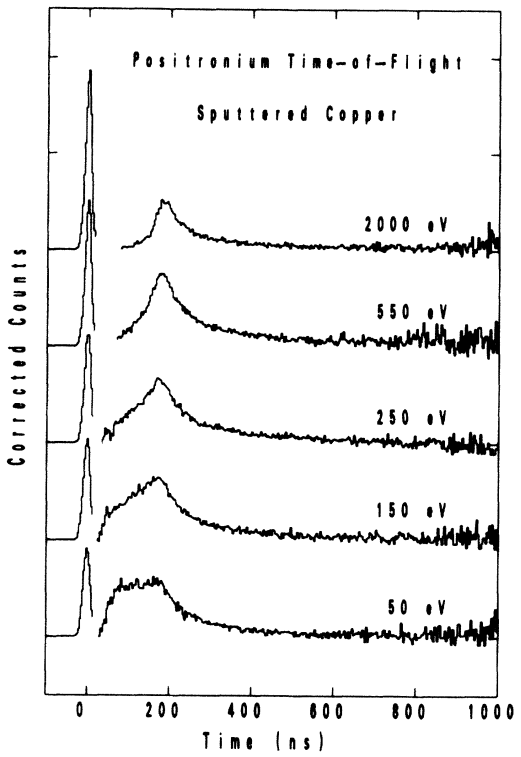

FIG. 4. Positronium time-of-flight spectra taken on sputter damaged Cu for energies between 2000 and 50 eV. Comparison of the spectra taken at 2000, 150, and 50 eV with those in Fig. 3, shows that the work-function positronium production is inhibited by sputtering. The backscatter positronium is insensitive to the sputter damage allowing the shape of the distribution of backscatter-formed positronium to be more easily seen.

The total backscattering probability depends on the elemental composition of the sample and the initial positron energy through the same scattering mechanism that determines the positron stopping profile. This results in higher probabilities for backscattering in elements with higher atomic number and weak dependence of the backscattering coefficient on the incident positron energy. Calculations of stopping profiles and backscatter energy spectra for positrons have been performed for positron energies above 2 keV (Ref. 5) for elements with low and high atomic numbers. While the inclusion of strong backscattering in the description of the slowing down process was a major improvement in these calculations, results for backscattering at positron energies below 2 keV were not reported. The energy spectrum of backscattered particles was calculated for positrons[5] and for electrons,[10] and while there was some backscatter strength in a smooth distribution at low positron energies, the most probable energy in the backscatter spectrum was always seen to be near the incident particle energy. The energy distribution of backscattered electrons or positrons can be qualitatively understood by considering that the mean free path for scattering in a solid is shortest near 60 eV and is much longer at higher and lower energies.[9] Thus, positrons at low or high energies can return to the surface after having undergone only a few scattering events. However, if the positron loses enough energy that the mean free path becomes significantly shorter, particles that reach the surface will have scattered many times and be smoothly distributed in energy down to near thermal energies. Near thermal energies, the mean free path becomes longer as the energy of the particle is decreased so that there is a corresponding increase in the flux at the surface at very low energies leading to thermalized positrons at the lowest energy.

The positronium formation from the backscattered positrons must include the energy dependence of the electron pickup probability at high energies. There are no direct measurements or calculations of high-energy positronium formation cross sections for atoms at a surface. Measurements have been performed in gases[11] and it was found that for most materials, the positronium-formation cross section had a maximum at positron energies near 10—30 eV, and diminished to low values above 100 eV. As an approximation, we assume that the overlap of the formation cross section with the tail of the scattered positron distribution from higher-energy positrons inhibits the formation of positronium with energies above 100 eV, and

results in a low-energy distribution of positronium that falls to background levels at a few eV.

In a measurement of the positronium energy spectrum formed from positrons passing through a thin carbon foil,[12] it was found that the positronium energy distribution had an $E^{-3/2}$ dependence. While these data are consistent with our observations, the positronium energy distribution is the combination of the effects of positron energy loss in the foil and the energy dependence of the electron pickup cross section. Since the positron transmission spectrum was not measured in the foil experiment, we can only note that the low-energy maximum in the positronium distribution in the foil experiment suggests that the electron pickup probability at the foil surface is similar to the atomic cross sections noted above.

A thermalized positron combining with an electron at the Fermi energy will result in positronium having the positronium work-function energy. Lower energy positronium can be produced from positrons at thermal or higher energies by the pickup of electrons bound deeper in the Fermi sea. The combination of these effects results in positronium produced in backscattering with a distribution extending from zero energy up to near the initial positron energy, but damped at high energies by the effects of the positronium formation cross section. At lower positron bombarding energies, the effects of the energy dependence in the production cross section are less important and positronium distributions have peaks at velocities much faster than those from work-function emission due to the low-energy structure in the backscattered positrons. Such a peak is missing in the smooth low-energy tail of the backscattering from high-energy positrons.

The shape of the backscatter-formed positronium distribution for low-energy positrons on samples with different densities and atomic numbers is similar for all the samples measured, as seen in Fig. 5. These spectra were taken with 50-eV positrons on annealed samples so that the work-function positronium has not been suppressed. In all of the samples, the backscatter process results in a peak at 10 ± 2 eV positronium energy with an edge at short times corresponding to a maximum positronium energy of more than 40 eV in all cases, suggesting that the positrons at this low energy undergo a small number of scattering events in reaching the surface. The variation among samples in the sharpness of the peak is probably due to the low initial positron energy allowing scattering differences to be preserved, since spectra taken at higher initial energies where the backscattered positron spectrum is expected to be featureless have similar shapes in the backscatter positronium.

The intensity of the positronium formed in backscattering has been determined from the time-of-flight spectra of Al, Cu, Ni, and Au for several energies. The backscattered intensity was calculated by summing the positronium from the work-function edge to a long-time cutoff at 400 ns and subtracting it from the total positronium summed from 25 to 400 ns. The work-function positronium was considered to be added to a backscatter contribution approximated by a linear extrapolation from the value at the high-energy side of the work-function peak, to zero at the time cutoff, as indicated by the shaded region in Fig. 3. The results of the positronium intensities are shown in Fig. 6. The integrated strength of the backscatter-formed positronium is normalized by the number of positrons incident on the sample. The ratio of positronium detected in the time-of-flight measurement, to positrons on the sample per unit charge of the linac electron beam, was determined using the prompt counting rate and the positronium fraction in the lifetime detector for measurements taken with a strongly attractive bias on the sample, i.e., < -50 V and high enough energy that the work-function mechanism was the dominant channel for positronium production.

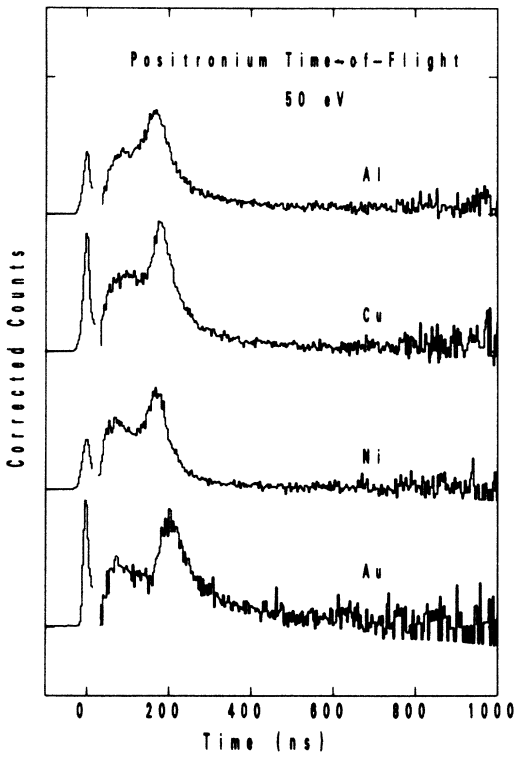

FIG. 5. Positronium time-of-flight spectra for clean, annealed samples of Al, Cu, Ni, and Au taken with 50-eV positrons. The general features of the spectra are similar, but there are differences in the distribution of the backscatter-formed positronium that are due to differences in the scattering of positrons from the samples.

The variation in the amount of backscattered positronium per eV change in incident positron energy for incident energies of 1 keV and above, is slow compared to the lower-energy data. The behavior at high incident energies is consistent with calculated strengths for electrons backscattering at similar energies over a similar range of materials.[9] In these calculations, a slowly-varying decrease in the scattering strength of electrons that lose most of their energy was predicted for incident energies above 500 eV.

At lower incident positron energies, the backscattering mechanism for producing positronium is stronger than at higher incident positron energies, and some variation with material is seen. The relative strength of the positronium formed from lower-energy positron beams is similar to the

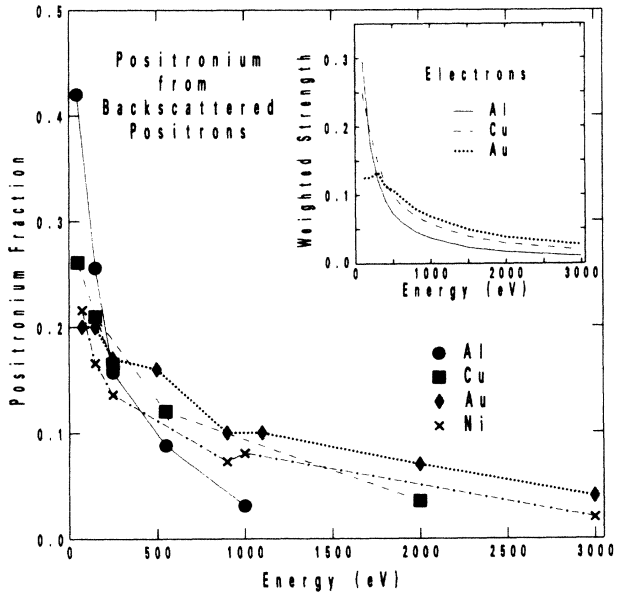

FIG. 6. Integrated strength of the backscattered positronium distribution for all spectra taken. The lower positronium strength at higher positron energies is due to the selection of a fixed low-energy part of the backscatter spectrum by the positronium formation cross section. The variations among samples are due to sample variations in backscattering probability and are similar to backscattering data for electrons (Ref. 13) weighted by $1/E$ as shown in the inset.

variation seen in total electron backscattering coefficients in the same initial energy range.[13] At 100-eV electron energy, Al has a greater backscatter coefficient than higher-Z materials; while at 1 keV, the Al backscatter coefficient is lower than those for Cu and Au. The strength of the electron backscatter coefficients is a maximum near 1-keV incident electron energy for all the materials in Ref. 10, while positronium production in backscattering is highest at lower (50 eV) incident positron energies. The source of this difference is the selection of lower-energy positrons from the backscatter spectrum by the energy dependence of the positronium production cross section. Thus, most low-energy positrons which subsequently backscatter, do so into an energy regime which is advantageous for producing positronium, while a proportionally smaller fraction of high-energy positrons scatter into that same energy region. The effect of selection of only positrons below some upper limit in positronium production can be approximated in the data of Ref. 10 by weighting the data by the inverse of the initial energy. These weighted data, shown in the inset in Fig. 6, normalized to the positronium production value for Al at 100 eV, are remarkably similar in their relative behavior to the positronium production data.

CONCLUSIONS

We have measured the velocity distributions of positronium emitted from single-crystal samples of Al, Cu, Ni, and Au after bombardment by positrons at several energies from 50 eV to 3 keV. The velocity distributions of the positronium demonstrate the existence of positronium produced through mechanisms that are controlled by the energetics of the positron and electron work functions and the binding energy of the positronium. In addition to the work-function positronium, a second positronium mechanism has been identified as positronium formed with positrons that scatter from the sample before thermalization. More positronium is produced from backscattered positrons than from diffusion-limited work-function positronium at low incident positron energies. The energetic positronium from the backscattered mechanism contributes an erroneous signal to defect depth profiling experiments which should have the effect of causing an underestimation of the defect concentration in the near-surface region. Combined with suitable depth profiling calculations and some knowledge of the positron-electron pickup cross section, suitable corrections could be made. Better yet, such experiments could be performed with the time-of-flight technique where the mechanisms are resolved. More importantly, it should now be possible, with suitable estimates of the implantation profile of the positrons, to extract information about the positron-electron pickup cross section from similar experiments.

The energy distribution of the backscatter positronium can be understood by considering that the mean free path for positrons is at a minimum in most materials at about 60 eV, allowing low-energy positrons to emerge from a material having lost energy in a small number of scattering events. Higher-energy positrons must undergo more interactions to scatter out so that the emerging positron energy spectrum is more uniform at low energies and little high-energy positronium is produced, due to the energy dependence of the positronium production cross section.

The integrated strength of the backscatter-produced positronium was determined for all of the samples in all of the spectra taken. The variation, due to changes in sample and positron energy in the strength of the backscatter positronium production, is consistent with the measured strength of backscattered electrons if the electron data are weighted by the inverse of the electron energy to approximate the selection of low-energy positrons by the energy dependence of the positronium production cross section.

ACKNOWLEDGMENTS

The authors would like to acknowledge valuable conversations with Risto Nieminen and Karl Canter. This work was performed at Lawrence Livermore National Laboratory supported by the U.S. Department of Energy under Contract No. W-7405-Eng-48.

[1]A. P. Mills, Jr., L. Pfeiffer, and P. M. Platzman, Phys. Rev. Lett. 51, 1085 (1983).

[2]A. P. Mills, Jr. and Loren Pfeiffer, Phys. Rev. B 32, 53 (1985); Phys. Rev. Lett. 43, 1961 (1979).

[3]K. G. Lynn, in *Positron Solid-State Physics,* edited by W. Brandt and A. Dupasquier (North-Holland, New York, 1983).

[4]A. P. Mills, Jr, P. M. Platzman, and B. L. Brown, Phys. Rev. Lett. 41, 1076 (1978).

[5]S. Valkealahti and R. M. Nieminen, Appl. Phys. A **32**, 95 (1983).

[6]W. Brandt, in *Radiation Effects on Solid Surface Advances in Chemistry,* Series 158, edited by M. Kaminsky (American Chemical Society, Washington D.C., 1976) pp. 219–244.

[7]R. H. Howell, M. J. Fluss, I. J. Rosenberg, and P. Meyer, Nucl. Instrum. Methods B **10**, 373 (1985).

[8]R. H. Howell, I. J. Rosenberg, M. J. Fluss, R. Goldberg, and R. Laughlin (unpublished).

[9]R. M. Nieminen and J. Oliva, Phys. Rev. B **22**, 2226 (1980).

[10]Arne L. Tofterup, Phys. Rev. B **32**, 2808 (1985).

[11]M. Charlton, Rep. Prog. Phys. **48**, 737 (1985); L. S. Fornari, L. M. Diana, and P. G. Coleman, Phys. Rev. Lett. **51**, 2276 (1983).

[12]A. P. Mills, Jr. and W. S. Crane, Phys. Rev. A **31**, 593 (1985).

[13]H. J. Fitting, Phys. Status Soldi A **26**, 525 (1974).